

# Spin Polarization of Gapped Dirac Surface States Near the Topological Phase Transition in $\text{TlBi}(\text{S}_{1-x}\text{Se}_x)_2$

S. Souma,<sup>1</sup> M. Komatsu,<sup>2</sup> M. Nomura,<sup>2</sup> T. Sato,<sup>2</sup> A. Takayama,<sup>2</sup>

T. Takahashi,<sup>1,2</sup> K. Eto,<sup>3</sup> Kouji Segawa,<sup>3</sup> and Yoichi Ando<sup>3</sup>

<sup>1</sup>WPI Research Center, Advanced Institute for Materials Research, Tohoku University, Sendai 980-8577, Japan

<sup>2</sup>Department of Physics, Tohoku University, Sendai 980-8578, Japan and

<sup>3</sup>Institute of Scientific and Industrial Research, Osaka University, Ibaraki, Osaka 567-0047, Japan

(Dated: June 4, 2019)

We performed systematic spin- and angle-resolved photoemission spectroscopy of  $\text{TlBi}(\text{S}_{1-x}\text{Se}_x)_2$  which undergoes a topological phase transition at  $x \sim 0.5$ . In  $\text{TlBiSe}_2$  ( $x = 1.0$ ), we revealed a helical spin texture of Dirac-cone surface states with an intrinsic in-plane spin polarization of  $\sim 0.8$ . Spin polarization still survives in the gapped surface states at  $x > 0.5$ , although it diminishes on approaching  $x = 0.5$  and vanishes in the non-topological phase. No evidence for the out-of-plane spin polarization was found irrespective of  $x$  and momentum. The present results unambiguously indicate the topological origin of the gapped Dirac surface states, and also impose a constraint on models to explain the origin of mass acquisition of Dirac fermions.

PACS numbers: 73.20.-r, 71.20.-b, 75.70.Tj, 79.60.-i

Three-dimensional topological insulators (TIs) exhibit a novel quantum state with metallic topological surface state (SS) which disperses across the bulk band gap generated by a strong spin-orbit coupling. Specifically, the topological SS is characterized by a linearly dispersing Dirac-cone energy band with the helical spin texture [1–4], which hosts massless Dirac fermions protected by time-reversal symmetry (TRS). The massless Dirac fermions in TIs provide a platform of fascinating quantum properties such as the robustness against non-magnetic impurities / disorder [5, 6] and the emergence of Majorana fermions [7]. Breaking the TRS by a magnetic field or a magnetic order lifts the band degeneracy at the Dirac point and causes an energy gap called a Dirac gap in the topological SS, turning the massless Dirac fermions into a massive state. Theoretically, realization of the massive state is a prerequisite for novel topological phenomena such as the topological magnetoelectric effect and half-integer quantum Hall effect [8, 9], but experimentally, the role of TRS-breaking magnetic impurities in triggering the Dirac-gap opening in the topological SS is under intense debate [10–13].

Recently, it was found by angle-resolved photoemission spectroscopy (ARPES) measurements that the thallium-based ternary chalcogenide solid-solution  $\text{TlBi}(\text{S}_{1-x}\text{Se}_x)_2$  goes through a quantum phase transition (QPT) from the topological ( $x > 0.5$ ) to the non-topological ( $x < 0.5$ ) phase [14, 15]. Intriguingly, the Dirac-cone topological SS in  $\text{TlBiSe}_2$  ( $x = 1.0$ ) starts to show a Dirac gap upon partially replacing Se with S, and the gap gradually grows on increasing the S content until the QPT at  $x = 0.5$  eliminates the SS [15]. Since there is no evidence for magnetic impurities in the measured crystals, it has been puzzling how the Dirac fermions in  $\text{TlBi}(\text{S}_{1-x}\text{Se}_x)_2$  acquire the mass without explicitly breaking the TRS. To gain insights into the microscopic mechanism of this

intriguing mass acquisition, it is of particular importance to establish the spin structure of the gapped SS in  $\text{TlBi}(\text{S}_{1-x}\text{Se}_x)_2$ , since the topological or non-topological nature of the SS as well as the origin of the Dirac gap is intimately related to the characteristics of the spin texture.

In this Letter, we report our spin-resolved ARPES results of  $\text{TlBi}(\text{S}_{1-x}\text{Se}_x)_2$  with various  $x$  values ( $x = 1.0, 0.9, 0.8, 0.6$ , and  $0.0$ ), and present the evolution of the spin texture as a function of  $x$ . We demonstrate that the helical spin texture persists even in the gapped SS observed at  $x > 0.5$ , while the spin polarization vanishes in the ARPES spectrum in the non-topological phase at  $x < 0.5$  in accordance with the absence of the SS. In addition, we found unusual reduction of the spin polarization in the SS near the QPT. We discuss the implications of the present experimental findings on the mechanism of the Dirac gap opening.

High-quality single crystals of  $\text{TlBi}(\text{S}_{1-x}\text{Se}_x)_2$  were grown by a modified Bridgman method. Details of the sample preparations were described elsewhere [15]. ARPES measurements were performed with a spin-resolved photoemission spectrometer based on MBS-A1 analyzer at Tohoku University [16]. We used one of the Xe I lines ( $h\nu = 8.437$  eV) to excite photoelectrons. Samples were cleaved *in situ* along the (111) crystal plane in an ultrahigh vacuum of  $5 \times 10^{-11}$  Torr. The energy resolution for the spin-resolved and regular ARPES measurements was set at 40 and 6 meV, respectively. The sample temperature was kept at 30 K during the measurements. We used the Sherman function value of 0.07 to obtain spin-resolved ARPES data [16].

First we demonstrate the spin structure of  $\text{TlBiSe}_2$  ( $x = 1.0$ ) in which the topological origin of the Dirac-cone SS is well established by previous studies [17–19]. Figure 1(a) shows the ARPES intensity plot at  $E_F$  of  $\text{TlBiSe}_2$

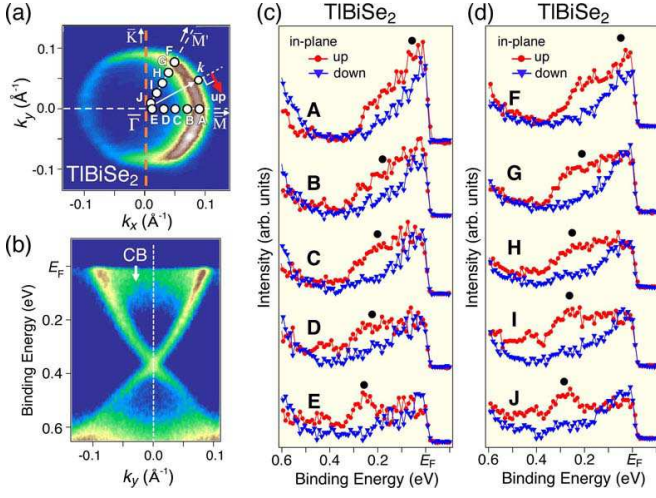


FIG. 1: (Color online) (a) ARPES intensity at  $E_F$  around the  $\bar{\Gamma}$  point for  $\text{TlBiSe}_2$  plotted as a function of two-dimensional wave vector  $\mathbf{k}$  measured with the Xe I resonance line ( $h\nu = 8.437$  eV) at  $T = 30$  K. The ARPES intensity is integrated within  $\pm 20$  meV with respect to  $E_F$ . The definition of an in-plane up-spin vector is also indicated by an arrow. (b) Near- $E_F$  ARPES intensity along the  $\bar{\Gamma}\bar{K}$  cut for  $\text{TlBiSe}_2$ . (c, d) Spin-resolved EDCs for the  $\mathbf{k}$  points (A-E and F-J) whose positions in the 2D Brillouin zone are indicated by open circles in (a).

around the  $\bar{\Gamma}$  point as a function of in-plane wave vector  $k_x$  and  $k_y$ . We clearly observe circular Fermi surface (FS) with hexagonal deformation, which originates from the upper branch of the Dirac-cone SS as displayed in Fig. 1(b). We also find a finite intensity distribution around the  $\bar{\Gamma}$  point as indicated by white arrow in Fig. 1(b). This signal is attributed to the bulk conduction band (CB) which is slightly occupied due to electron doping caused by Se vacancies in the crystals [17–19].

Figures 1(c) and (d) show spin-resolved energy distribution curves (EDCs) of  $\text{TlBiSe}_2$  for the in-plane spin component measured at various  $\mathbf{k}$  points along the  $\bar{\Gamma}\bar{M}$  cut as indicated in Fig. 1(a). We define the spin polarization vector perpendicular to the measured  $\mathbf{k}$  [see, e.g., thick red arrow in Fig. 1(a)], where the “up spin” points to the clockwise direction. One can immediately recognize that the up-spin EDC is always more prominent than the down-spin counterpart in all the measured  $\mathbf{k}$  region, consistent with the spin helical texture of the Dirac-cone SS [4, 14]. Upon closer look, one finds that the shape of the up-spin EDC depends on the  $\mathbf{k}$  point. For instance, near the  $\bar{\Gamma}$  point (point E and J) the peak in the up-spin EDC (marked by circle) is located at  $\sim 0.3$  eV, but it approaches  $E_F$  on moving away from the  $\bar{\Gamma}$  point (from E to A, or from J to F), reflecting an electronlike dispersion of the upper branch of the Dirac cone (note that the dispersive feature is less clear than the regular ARPES data because of the wider  $\mathbf{k}$  window and the lower energy resolution of the spin-resolved mode). On

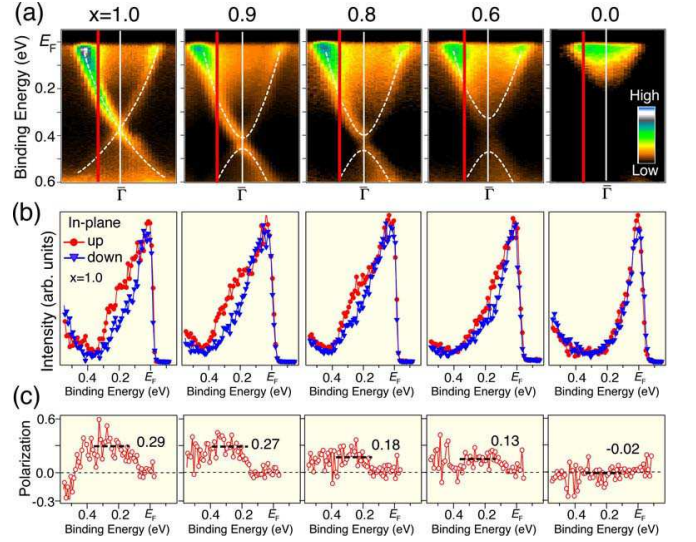


FIG. 2: (Color online) (a)  $x$ -dependence of near- $E_F$  ARPES intensity around the  $\bar{\Gamma}$  point for  $\text{TlBi(S}_{1-x}\text{Se}_x)_2$ . Dashed lines are guides to the eyes to trace the band dispersion. The vertical red (thick) line represents the  $\mathbf{k}$  point where the spin-resolved EDCs were obtained. (b, c) Corresponding spin-resolved EDCs for the specified  $\mathbf{k}$  point and their spin polarization  $P_{\text{IP}}$ , respectively. In (c), the averaged  $P_{\text{IP}}$  value in the energy window of  $\pm 0.1$  eV with respect to the energy of the SS ( $E_{\text{SS}}$ ) is indicated by a number and also by a dashed line. The experimental uncertainty (error bar) in the averaged  $P_{\text{IP}}$  value is  $\pm 0.05$ .

the other hand, the peak in the down-spin EDC is always pinned at  $E_F$ . This is because it is governed by the bulk CB which contributes equally to the up- and down-spin EDCs around the  $\bar{\Gamma}$  point (as evidenced by the small difference in the near- $E_F$  spectral weight between the up- and down-spin data at points D, E, I, and J) as a result of the spin-degenerated character.

Figure 2(a) shows the near- $E_F$  ARPES intensity plot of  $\text{TlBi(S}_{1-x}\text{Se}_x)_2$  measured along the  $\bar{\Gamma}\bar{M}$  direction ( $k_x$ ) for various  $x$  values ( $x = 1.0-0.6$  in the topological phase and  $x = 0.0$  in the non-topological phase). The “X”-shaped topological SS transforms into the gapped SS in  $x = 0.9-0.6$ , as one can see from the suppression of the ARPES intensity at the Dirac point and the parabolic-like dispersion of the upper branch of the Dirac cone. At  $x = 0.0$  ( $\text{TlBiSe}_2$ ), the SS completely disappears and only the bulk CB is observed at  $E_F$ , reflecting the non-topological nature [15].

To elucidate the evolution of the spin structure of the SS, we have performed spin-resolved ARPES measurements by focusing on a particular  $\mathbf{k}$  point. The  $\mathbf{k}$  point was chosen to be located midway between the Fermi vector ( $k_F$ ) and the  $\bar{\Gamma}$  point along the  $\bar{\Gamma}\bar{M}$  direction [see vertical red (thick) line in Fig. 2(a)] so that the binding energy ( $E_B$ ) of the surface band ( $E_{\text{SS}} \sim 0.25$  eV) is apart from that of the bulk CB. As can be seen in Fig. 2(b), the shape of the spin-resolved EDCs for the in-plane compo-

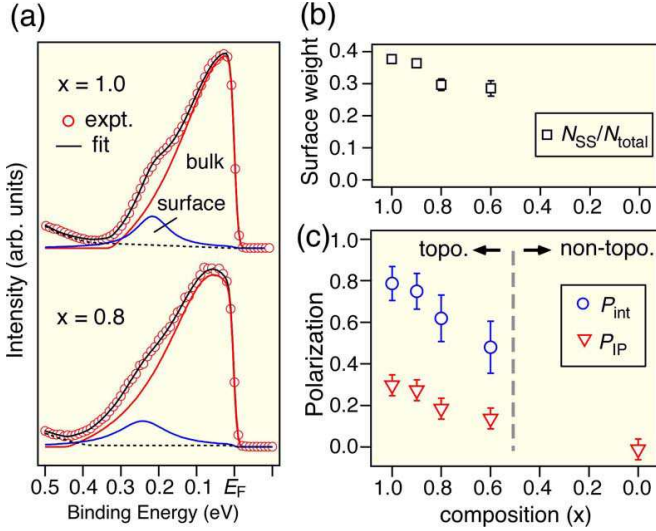


FIG. 3: (Color online) (a) Representative results of the two-component fitting to the EDC obtained by the regular ARPES experiment to estimate the bulk and surface spectral weights as indicated by blue and red curves, respectively. The plotted EDCs are generated by summing the raw EDCs within the  $\mathbf{k}$  window of the spin-resolved measurement, to take into account the  $\mathbf{k}$  broadening effect. In the fitting, we assumed a Lorentzian peak for the surface, bulk VB, and bulk CB, multiplied by the Fermi-Dirac distribution function. A constant term was subtracted from the peaks for bulk VB and CB to reproduce the bulk band gap. (b) Ratio of the surface spectral weight to the total spectral weight,  $N_{SS}/N_{total}$  (where  $N_{total} = N_{SS} + N_{bulk}$ ), at  $E_{SS}$  plotted against  $x$  as estimated by the fitting of EDCs [see Fig. 3(a)]. (c)  $P_{IP}$  divided by  $N_{SS}/N_{total}$ , which represents the intrinsic spin polarization  $P_{int}$  of the SS (circles).  $P_{IP}$  is also plotted with triangles.

ment is similar between  $x = 1.0$  and  $0.9$ . In addition, the spin polarization ( $P_{IP}$ ) [Fig. 2(c)] exhibits a similar value of  $\sim 0.3$ , suggesting that the gapped SS in  $x = 0.9$  has a helical spin texture as in  $x = 1.0$ . Another notable aspect is that the in-plane spin polarization is gradually reduced on approaching the QPT at  $x \sim 0.5$ , as evidenced by the smaller difference between the up- and down-spin EDCs for the samples with lower  $x$  values. The  $P_{IP}$  value in  $x = 0.6$  is  $\sim 0.15$  (half of that at  $x = 1.0$ ), and it vanishes in the non-topological phase ( $x = 0.0$ ).

To discuss more quantitatively the absolute spin polarization of the SS, it is necessary to remove the finite contribution from the spin-degenerated bulk band. For this purpose, we have fit the EDCs in the regular ARPES measurement by incorporating both the surface and bulk components [see Fig. 3(a)], and estimated the spectral weight of the SS ( $N_{SS}$ ) with respect to that of the total weight ( $N_{total} = N_{SS} + N_{bulk}$ ). The intrinsic in-plane spin polarization of the SS ( $P_{int}$ ) corresponds to the  $P_{IP}$  value divided by  $N_{SS}/N_{total}$ . Figures 3(b) and (c) display the  $x$ -dependence of  $N_{SS}/N_{total}$  and  $P_{int}$  ( $P_{IP}$  is also plotted for reference), respectively. As can be seen in Fig.

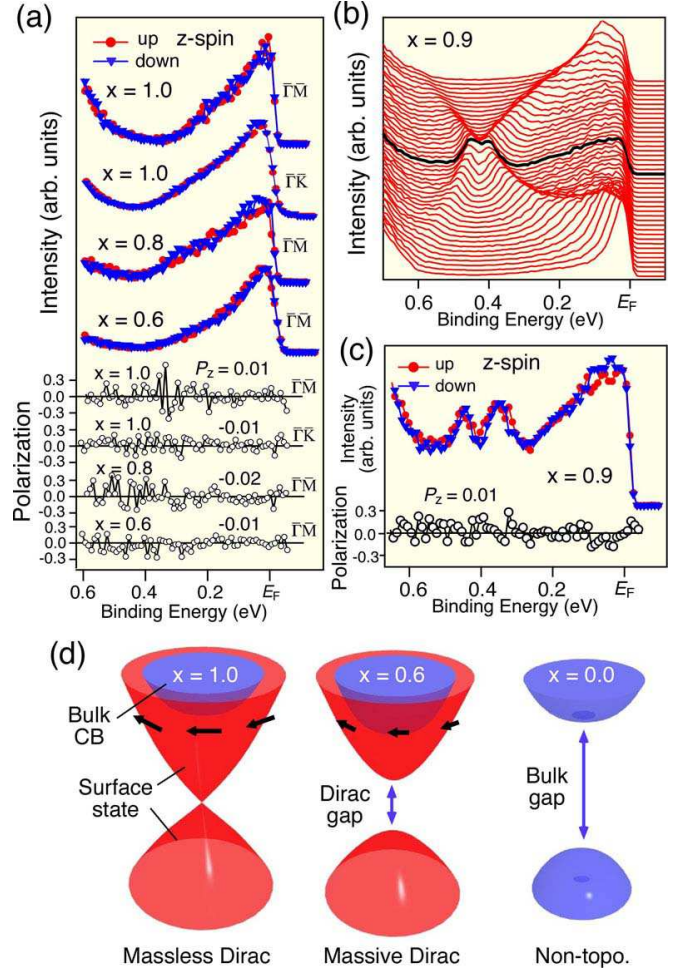


FIG. 4: (Color online)(a) Spin-resolved EDCs and corresponding spin polarization for the out-of-plane component in the topological phase ( $x = 1.0, 0.8$ , and  $0.6$ ) measured at the  $\mathbf{k}$  point along the  $\bar{\Gamma}\bar{M}$  direction indicated by the red (thick) line in Fig. 2(a). The EDCs along the  $\bar{\Gamma}\bar{K}$  direction are also plotted for  $x = 1.0$ . (b) Near- $E_F$  EDCs for  $x = 0.9$ . Spectrum at the  $\bar{\Gamma}$  point is highlighted by thick black curve. (c) Spin-resolved EDCs and corresponding spin polarization for the out-of-plane component measured at the  $\bar{\Gamma}$  point for  $x = 0.9$ . (d) Schematic picture of the evolution of the topological SS (red) and bulk bands (blue) as a function of  $x$ . The spin polarization vector is indicated by black arrows.

3(c), the estimated  $P_{int}$  value, which reaches  $\sim 0.8$  for  $x = 1.0$ , is gradually reduced on increasing  $x$  to reach  $\sim 0.5$  at  $x = 0.6$ , and finally vanishes in the non-topological phase at  $x = 0.0$ . The origin of the reduction in the in-plane spin polarization toward the QPT in the gapped SS is not clear, but the less-than-unity value of  $P_{int}$  at  $x = 1.0$  is likely to be a consequence of the spin-orbit entanglement as proposed from first-principle calculations [20].

The next important issue to clarify is the out-of-plane ( $z$ ) spin component. Figure 4(a) displays the spin-resolved EDCs and corresponding spin polarizations for



the  $z$ -spin component measured at the same  $\mathbf{k}$  point as in Fig. 2 (along the  $\bar{\Gamma}\bar{M}$  direction) for the samples in the topological phase ( $x = 1.0, 0.8$ , and  $0.6$ ). Spin-resolved EDCs for the  $\mathbf{k}$  point along the  $\bar{\Gamma}\bar{K}$  direction are also displayed for  $x = 1.0$ ; obviously, there is no apparent  $z$ -spin component in the  $\bar{\Gamma}\bar{M}$  nor the  $\bar{\Gamma}\bar{K}$  directions. It was previously found [4, 21, 22] that in  $\text{Bi}_2\text{Te}_3$  a finite  $z$ -spin texture emerges along the  $\bar{\Gamma}\bar{K}$  direction due to strong hexagonal warping of the SS. However, the hexagonal warping effect is much weaker in  $\text{TlBi}(\text{S}_{1-x}\text{Se}_x)_2$  than in  $\text{Bi}_2\text{Te}_3$ , resulting in no or negligible  $z$ -spin component [4]. The present data reconfirms this previous result for the whole topological phase, where the estimated  $z$ -axis spin polarization remains negligible ( $-0.02 \sim +0.01$ ).

While the above result demonstrates no  $z$ -spin polarization near the  $k_F$  point, a natural question arises as to whether any  $z$ -spin component exists exactly at the  $\bar{\Gamma}$  point. To address this issue, first we carefully examined the EDCs for  $x = 0.9$  [Fig. 4(b)] and determined the spectrum which exactly corresponds to the  $\bar{\Gamma}$  point (thick line), and then performed the spin-resolved ARPES measurement at this  $\mathbf{k}$  point with a higher energy resolution (15 meV). As shown in Fig. 4(c), we have succeeded in resolving two well-separated peaks in the spin-resolved EDCs attributed to the upper and lower branches of the gapped SS, respectively. Notably, there is essentially no difference between the up- and down-spin EDCs, indicating null  $z$ -spin polarization. These results suggest that the  $z$ -spin component is absent irrespective of  $x$  and  $\mathbf{k}$ . Based on these observations, we depict in Fig. 4(d) the schematic picture of the spin-texture evolution for three different phases (massless Dirac, massive Dirac, and non-topological phases) in  $\text{TlBi}(\text{S}_{1-x}\text{Se}_x)_2$ .

Now we discuss the implications of the observed characteristics of the spin polarization in relation to the Dirac-gap opening. First, the present result directly addresses the question whether the gapped SS has a topological origin. One may argue that the topological phase transition should have occurred between the massless ( $x = 1.0$ ) and the massive ( $x = 0.9$ ) phase, and that the observed gapped SS corresponds simply to a pair of trivial, spin-degenerate SSs which happened to present a gap-like feature at the  $\bar{\Gamma}$  point. In this respect, such a possibility is immediately ruled out by the observation of the spin non-degenerate nature of the gapped SS.

Another possible origin of the gapped SS is the hybridization of two topological SSs. In ultrathin films of  $\text{Bi}_2\text{Se}_3$ , it was reported that a Dirac gap opens when the electron wavefunctions of the top and bottom surfaces start to hybridize [23, 24]. In this case, the hybridized state is spin degenerate and loses the original helical polarization [25]. While the thick nature of our samples ( $\sim 100 \mu\text{m}$ ) already spoke against this possibility [15], the spin non-degeneracy observed here conclusively rules out the hybridization scenario. Moreover, a recent theory for ultrathin films in the hybridized state predicted a finite

$z$ -spin component [24], which was not observed in the present experiment.

An important question is whether the TRS is broken in the massive Dirac phase. When the topological SS feels a magnetic field or magnetization directed perpendicular to the surface (along the  $z$ -axis), it obtains a Dirac gap and the spin vector at the  $\bar{\Gamma}$  point is aligned along the  $z$ -axis in opposite directions in the lower and upper branches of the gapped SS [9]. In this respect, our finding that there is no  $z$ -spin component in the gapped SS does not give any support to this scenario. Nevertheless, one should keep in mind that if there are magnetic domains with antiparallel polarizations, the overall  $z$ -spin component can be canceled. Hence, it is difficult to draw any firm conclusion about the TRS breaking from the present experiment.

A viable possibility for the origin of the Dirac gap is the bulk-surface coupling. A recent theory suggested that the Dirac-cone feature can be destroyed by strong potential impurities which lead to bulk-assisted scattering to allow virtual spin-flip excitations [26]. The proximity of the bulk band to the Dirac point near the QPT [15] and the disorder due to random replacement of S with Se may be in line with this scenario. Another possibility could be critical fluctuations associated with the QPT as mentioned in Ref. [15], and the reduction of the net spin polarization toward the QPT may be in line with this scenario; however, no evidence for such critical fluctuations has been obtained so far. While a comprehensive answer to the origin of the Dirac gap has not yet been obtained, the present observation that established the nature of the spin texture and its evolution in the gapped phase provides an important step toward microscopic understanding of the topological QPT and the unconventional mass acquisition of Dirac fermions in TIs.

In summary, we have reported our spin-resolved ARPES experiments on  $\text{TlBi}(\text{S}_{1-x}\text{Se}_x)_2$  to determine the spin polarization as a function of  $x$ . We found that the helical spin texture survives in the massive Dirac phase, which clearly points to the topological nature of the gapped SS. While the exact mechanism of the Dirac gap opening is yet to be elucidated, the direct connection between the emergence of the helical spin texture and the topological QPT, as well as the reduction of the net spin polarization toward the QPT, gives an important clue.

We thank K. Kosaka and T. Arakane for their assistance in ARPES measurements, and T. Minami for his help in sample preparations. This work was supported by JSPS (NEXT Program and KAKENHI 23224010), JST-CREST, MEXT of Japan (Innovative Area “Topological Quantum Phenomena”), AFOSR (AOARD 104103 and 124038), and KEK-PF (Proposal number: 2012S2-001).

- 
- [1] M. Z. Hasan and C. L. Kane, Rev. Mod. Phys. **82**, 3045 (2010).
  - [2] X.-L. Qi and S.-C. Zhang, Rev. Mod. Phys. **83**, 1057 (2011).
  - [3] Y. Xia *et al.*, Nature Phys. **5**, 398 (2009).
  - [4] S. Souma *et al.*, Phys. Rev. Lett. **106**, 216803 (2011).
  - [5] A. A. Taskin, S. Sasaki, K. Segawa, and Y. Ando, arXiv:1204.1829.
  - [6] J. Seo *et al.*, Nature (London) **463**, 343 (2010).
  - [7] L. Fu and C. L. Kane, Phys. Rev. Lett. **100**, 096407 (2008).
  - [8] X.-L. Qi *et al.*, Science **323**, 1184 (2009).
  - [9] X.-L. Qi, T. L. Hughes, and S.-C. Zhang, Phys. Rev. B **78**, 195424 (2008).
  - [10] Y. L. Chen *et al.*, Science **329**, 659 (2010).
  - [11] T. Valla, Z. H. Pan, D. Gardner, Y. S. Lee, and S. Chu, Phys. Rev. Lett. **108**, 117601 (2012).
  - [12] M. R. Scholz *et al.*, arXiv:1108.1037.
  - [13] L. A. Wray *et al.*, Nature Phys. **7**, 32 (2010).
  - [14] S.-Y. Xu *et al.*, Science **332**, 560 (2011).
  - [15] T. Sato *et al.*, Nature Phys. **7**, 840 (2011).
  - [16] S. Souma *et al.*, Rev. Sci. Instrum. **81**, 095101 (2010).
  - [17] T. Sato *et al.*, Phys. Rev. Lett. **105**, 136802 (2010).
  - [18] Y. L. Chen *et al.*, Phys. Rev. Lett. **105**, 266401 (2010).
  - [19] K. Kuroda *et al.*, Phys. Rev. Lett. **105**, 146801 (2010).
  - [20] O. V. Yazyev, J. E. Moore, and S. G. Louie, Phys. Rev. Lett. **105**, 266806 (2010).
  - [21] Y. H. Wang *et al.*, Phys. Rev. Lett. **107**, 207602 (2011).
  - [22] S.-Y. Xu *et al.*, arXiv:1101.3985.
  - [23] Yi Zhang *et al.*, Nature Phys. **6**, 584 (2010).
  - [24] H.-Z. Lu, W. Y. Shan, W. Yao, Q. Niu, and S. Q. Shen, Phys. Rev. B **81**, 115407 (2010).
  - [25] A. Takayama *et al.*, Nano Lett. **12**, 1776 (2012).
  - [26] A. M. Black-Schaffer and A. V. Balatsky, Phys. Rev. B **85**, 121103(R) (2012).